Dynamics of subrelativistic electron beams in the solar corona

Type III group analysis

A. Hillaris[1], C.E. Alissandrakis[2], J-L. Bougeret[3], and C. Caroubalos[4]

[1] Section of Astrophysics, Astronomy and Mechanics, Department of Physics, University of Athens, GR-15784 Athens, Greece
   (e-mail: ahilaris@atlas.uoa.gr)
[2] Section of Astro-geophysics, University of Ioannina, GR-45110 Ioannina, Greece
[3] Observatoire de Paris, Department de Recherche Spatial, CNRS UA 264, F-92195 Meudon Cedex, France
[4] Department of Informatics, University of Athens, GR-15783 Athens, Greece

Abstract. A number of type III groups is studied. Wave particle interactions are neglected and the so called drift approximation is used to model the electron beam evolution. We extrapolated the observed Flux-Time profiles towards higher frequencies and estimated the injection time for the individual beams responsible for the excitation of the type III's. A simple *clustering algorithm*, based on the temporal separation of nearest neighbour injections as a proximity criterion, was used to identify patterns of burst subgroups within the type III groups. The question of whether the acceleration and injection of component bursts exciters is coherently modulated in a single source, or this process is driven by a statistical flare in a spatially fragmented energy release site, is addressed.

Key words: Sun: activity – Sun: corona – Sun: radio radiation

1. Introduction

Radio bursts of the type III family are produced by energetic electrons accelerated in the Sun and traversing the solar atmosphere, moving along magnetic lines rooted in these regions (Wild 1950). Only a very small number of type III events appear isolated on the dynamic spectra. The time profile of such an isolated event at a given frequency is believed to represent the passage of a single electron beam (Type III exciter) through that plasma frequency level; the decay part is almost exponential, while the rising part is slightly steeper than the decaying. The burst duration at each level is believed to be related to the duration of the excitation (i.e. the time required for the exciter to cross the level) rather than the response of the medium; it increases with time, which indicates an increase of the exciter length with the distance traversed by the beam due to dispersion (Poquerusse et al., 1984).

More often than not, type III events appear in groups and storms of ten or more bursts. The hypothesis that they frequently show quasi periodic behavior (Wild 1963) has produced some

Send offprint requests to: A. Hillaris

controversy Mangeney and Pick (1989) and Zhao et al. (1991) Fourier analyzed differentiated time series of type III events and based their results on the observed spectral peaks which they considered as evidence of a periodic process with a repetition rate of about two bursts per second. However, Isliker (1996) pointed out that the peaked power spectrum can be the signature of a stochastic process as well, since he obtained qualitatively similar results by analyzing a random pulse series of about 15 pulses. Aschwanden et al. (1990, 1993, 1994, 1995) observed sequences of associated hard X-ray (HXR) and radio bursts, which were both found to be quasi-periodically organized with periods of 2.1 ± 1.0 s. They also noted that the pulse duration of correlated bursts was about 0.8 ± 0.4 s in radio and 1.0 ± 0.7 s in HXR. Based on these results they introduced the *pulsed mode* hypothesis:

The *pulsed mode* hypothesis implies a large scale mechanism, responsible for the modulation of the beam injection affecting the whole active region. Aschwanden et al. (1994) used the ratio, λ, of the standard deviation to the average periodicity (inter arrival time between pulses, $\delta\tau$) as a criterion; they found that it is significantly smaller than unity (less than 49% on the average, compared to more than 67% in an artificial random time series) and they concluded that the event occurrence is more of a periodic than of a random nature. Based on these they suggest that the duration and periods of burst groups are characteristic of the intrinsic time scale of a common bidirectional injection and/or acceleration mechanism where upward injected electrons excite the type III bursts and downward electrons the HXR pulsations. The ratio of pulse duration to pulse interval, which was found in all cases to be about 50%, suggests an oscillation controlled injection/acceleration mechanism. These results were criticized by Yurovsky and Magun (1996) who point out that the *pulsed* mechanism proposed by Aschwanden et al (1994) cannot be attributed into any *resonant system* because the system *quality*, Q, is too small (Q≈1); moreover, the almost exponential distribution of inter arrival times between subsequent pulses implies a random accelerator with Poisson statistics. Furthermore Isliker (1996) argued that

temporal correlations in examined time series cause the relative spread of the parameter λ to take a broad range of values which render it inadequate as a quasi-periodicity criterion, since the ranges for periodic and stochastic behavior overlap considerably.

The *fragmented acceleration site model* on the other hand (suggested by Vlahos, 1991, 1993, 1994), involves a large number of magnetic structures; the components of the type III group are excited by electrons propagating along different flux tubes, each rooted to a source element (Benz et al., 1982; Pick & Van Den Oord, 1990; Roelof & Pick, 1989). Simulations by Vlahos & Raoult (1995) show that beam injections into independent coronal fibers can account for the observed flux-time profiles of type III groups. The physics in the source of such groups is believed to be intimately related with the concept of the *statistical flare* which is characterized by spatial and temporal fragmentation and clustering of an active region in small and large scale structures (Bastian and Vlahos, 1996). The clustering of many discontinuities (i.e. small scale magnetic structures) in the same area has the effect of larger scale explosions (statistical flares) by means of an avalanche process, where local energy release may either energize (add free energy) or trigger the explosion of neighboring structures (each resulting in a microflare, in which the released energy is well below the observational threshold) which in turn may affect similarly their own neighbors. Vlahos et al., (1995) (also MacKinnon et al 1996), modeled the energy release process by a cellular automaton *avalanche* system which evolves towards *self organized criticality* under random initial perturbations (see also Lu and Hamilton 1991, Lu at al 1993, Georgoulis and Vlahos, 1996), in an attempt to interpret the observed energy and duration distributions. A major advantage of this approach is that detailed knowledge of the elementary acceleration mechanism is not required, hence conclusions remain valid for a multitude of candidate energy release and particle acceleration processes. The results of these simulations provide a basis for the interpretation of the well established observational result that production of energetic particles occurs in a complex magnetic environment, where organized building of successive elementary releases in many different magnetic structures is expected (Vilmer and Trottet, 1996).

One of the principal observational difficulties is the identification of the start time of each beam injection; the use of the peak times of type III component bursts at a particular frequency is not adequate, since individual beams may have evolved in a different way in their course from their source to that level. In this article we use theoretical analytic expressions for isolated type III flux-time profiles (Hillaris et al 1990), to decompose the group into a superposition of component bursts. These component bursts are extrapolated downwards, towards higher frequencies, and the injection time for each of them is calculated. The interval between successive components is used as a criterion for the identification of clusters within the main type III group. It is noted in passing that no assumption is made about the clusters, which are identified on the basis of measurements of time interval between consecutive injections (inter arrival time). The comparative study of clusters is used for the investigation

of whether acceleration and injection of the beams is coherently modulated in a single source, or whether this process is driven by the statistical flare mechanism.

In the next section we discuss the dynamics of an electron beam and the model of the flux-time profile at various distances from the injection site, corresponding to different heights in the corona, which simulates the radio flux-time profile of an isolated type III event or a component of a group. In Sect. 3 we present the basics of the clustering algorithm which is used to identify a hierarchy of subgroups within the main type III group. In Sect. 4 we give a brief description of the observations and the data reduction process. In Sect. 5 we use the model to separate the components of four type III groups, observed with the Multichannel Radiospectrograph of the Space Research Laboratory of the Observatory of Paris (RSMN), (Dumas et al., 1982). The flux-time profiles of each component are extrapolated towards higher frequencies, to identify the injection time for each. Subsequently the clustering algorithm is applied to each group in order to identify a hierarchy of subgroups within it. The results of this analysis, conclusions and suggestions for further study are discussed in Sects. 6 and 7 respectively.

2. Model of the type III flux-time profile

Type III bursts are believed to be produced by electron beams propagating over large distances along open or closed magnetic field lines and exciting Langmuir waves via the beam-plasma instability. The problems that should be addressed first are the stabilization of the beam as well as how the Langmuir waves drive the electromagnetic radiation. Once the relationship between the electron beam evolution and the observed electromagnetic radiation is established, one can infer the initial exciter characteristics from the observations and subsequently attempt an analysis of the acceleration site physics.

A model for the non-linear beam stabilization, propagation and electromagnetic emission for type III events has been proposed and applied by Hillaris et al (1988, 1990). This model was based on the Langmuir-ion acoustic wave coupling via the ponderomotive force (Zakharov 1972) which can efficiently transfer Langmuir wave energy out of resonance with the streaming electrons, to secondary Langmuir modes and ion acoustic waves, thus stabilizing the type III exciter (Papadopoulos 1975; Papadopoulos et al., 1974, Smith et al, 1979, Goldstein et al 1979). The stabilization process is further enhanced by Langmuir wave scattering on ion acoustic waves (Dawson and Oberman 1962) as well as by scattering on density irregularities and ion acoustic waves already present.

The non linear, wave-wave interactions, not only can stabilize the exciter by almost suppressing the growth of the resonant Langmuir wave (Vlahos & Rowland, 1984) but can also provide an emission mechanism for the electromagnetic radiation. At twice the plasma frequency, emission results from the head on collision of counter streaming secondary Langmuir modes with almost equal wave numbers. At the plasma frequency, on the other hand, by the Langmuir-ion acoustic wave interaction (cf. Papadopoulos & Freud 1979). Simulations by Hillaris et

al. (1988) show that the radiation light curves (Electromagnetic wave flux time profiles) at a given distance from the injection site have a power law dependence on the exciter local density, therefore the logarithmic profile of the exciter density as a function of time (exciter density-time profile) at a given level represents the event light curve at this level (cf. Eq. 1 below). This was used by Hillaris et al (1990), in the analysis of isolated type III and J events obtained with the Multichannel Radiospectrograph of the Space Research Laboratory of the Observatory of Paris (RSMN) with a time resolution of 1/10 sec.

On the basis of the above discussion, the exciter of a type III event will loose a small percentage of its energy to the Langmuir waves of the beam-plasma instability, so its propagation can be modelled by a free streaming distribution with only a collision term. This term, in our model, is of the Krook type (Bhatnagar et al 1954) including both Coulomb and particle-ion density fluctuation collisions (Papadopoulos 1977). The latter makes the collision term dominant over particle diffusion in velocity space which is ignored. The radiation flux (F) was found by simulations to be:

$$F(x,t) \propto \left(\frac{n_b}{n_a}\right)^\delta = \left(\frac{1}{n_a}\int f_b(x,v,t)dv\right)^\delta \qquad (1)$$

where n_a is the ambient plasma density, n_b the beam density, $f_b(x,v,t)$ the exciter electrons distribution, and the power law index δ was found to be about 2 (Hillaris et al 1988, 1990).

For an initial (i.e. at $t = t_0$) exciter distribution in the form of a super hot electron component, we can have an analytical expression of the temporal and spatial evolution of the exciter electrons $f_b(x,v,t)$ of the type:

$$\begin{aligned} f_b(x,v,t) &= f_b(x - v\tau, v, \tau = 0)e^{-\gamma_{eff}\tau/v^3} \\ &= n_0 e^{-(v/\delta v)^2} e^{-((x-v\tau)/\delta x)^2} e^{-\gamma_{eff}\tau/v^3} \end{aligned} \qquad (2)$$

where $\nu_{eff} = \gamma_{eff}/v^3$ is the effective collision frequency, δv the velocity dispersion of the super thermal population, δx the length of original spatial dispersion of the exciter and $\tau = t - t_0$.

The time-profile of the beam density, $n_b(x,t)$, and the radiation flux, F(t), at various distances from the injection site, i.e. at various local plasma frequencies, is thus obtained by integration of Eq. (2) over velocity. Substituting the result of the integration into (1) the form of the flux (F)-time profile, for very small δx, is:

$$\log_{10} F(t) = A - \alpha \ln(t - t_0) - \beta(t - t_0)^{-2} - \gamma(t - t_0)^{-3} \qquad (3)$$

The free parameters, $A, \alpha, \beta, \gamma, t_0$, which define the shape of the burst profile, depend on the injection characteristics, the power law index in Eq. (1) and the distance, x, from the injection site corresponding to the frequency of observation, as well as the units in which the flux is measured. They are estimated by fitting Eq. (3) to the undisturbed part of the observed radio flux-time profiles as described in Sect. 5. In this report we normalize the $\log_{10} F$-time profile at each frequency to the maximum for that frequency and use units of 1/50 db's.

3. Cluster detection in type III groups

3.1. Hierarchical clustering in type III groups

Cluster analysis is the process of classifying objects into subsets that have meaning in the context of a particular problem. The algorithms for this type of classification, known as clustering algorithms, group objects based on the index of proximity between pairs of them. This is a measure of alikeness, or affinity, or association, established between pairs of different objects and is the basis of every clustering method (Jain and Dubes 1988). A dissimilarity index can be used as well; in this case the smaller the index between a pair the more its members resemble each other. Distance is of the most common examples of such a dissimilarity index. A similar classification scheme based on Euclidean distance has been applied for decameter solar type III bursts by Stepanova et al (1995) on a 1000 burst sample. However, the parameters used by them in the distance calculation are the time delay between successive bursts, half-intensity duration, maximum intensities for left and right polarized wave, and degree of circular polarization, since they attempt to detect classes of type III bursts which can be associated with different components of type III radiation (F, H, etc.).

In this report the objects (also met as cases, subjects or operational taxonomic units in the literature, cf. Jain & Dubes, 1988), are component bursts which form a type III group. The dissimilarity index is computed from the data at hand, and in this case is the difference of the injection time (estimated as described in Sect. 5) between any two bursts. Since the beginning of the measurement of time can be selected arbitrarily, only the time intervals are meaningful in this analysis and our indices are said to be on an interval scale.

The *proximity matrix* formed by the indices, i.e. the matrix $[\delta t_{ij}]$ where δt_{ij} is the interval between the i-th and j-th component bursts, is the one and only input to the clustering algorithm. This results in an intrinsic classification of the data and does not assume anything about the nature of the clusters, so that the only thing requiring a thorough examination of the nature of the problem is the selection of the association criterion. In this case the dissimilarity index almost suggests itself, since it is chains of successive bursts within a group that we want to analyze.

Groups of type III bursts consist of subgroups which may have a fine structure of their own. In this context, detecting and identifying nested partitions of subgroups, which define the so called hierarchical clustering, seems appropriate while, in addition, no assumption about the number of clusters is required as would be the case in partitional clustering. Partitional clustering generates a single partition of the data in an attempt to recover natural groups. To this end a clustering criterion has to be adopted such that data points (also referred to as patterns) in a cluster are more similar to one another than patterns in different clusters. Thus the criterion imposes a certain structure on the data and introduces a dependency between the clustering method and the type of cluster expected. In our case, the clustering criterion could have been the adoption of a certain interval between nearest neighbors as the upper bound for cluster formation, so that each event exceeding this limit would start

a new cluster. However, such an assumption is not made here since we are interested in a hierarchy of clusters rather than in any single partition.

The proximity matrix for each type III group of n components, once calculated, is used as a $n \times n$ symmetric adjacency matrix for the construction of an undirected weighted graph, $G(n)$, on n nodes, each representing a component burst of the group. The weight of each link of the graph is equal to the dissimilarity index (difference of injection times) of the adjacent nodes. We proceed in the cluster detection by removing all links with dissimilarity indices greater than some threshold, d, for the graph, forming thus the threshold graph $G(n, d)$ of $G(n)$. At each stage of the process, as we decrease the threshold d, the connected sub graphs of $G(n, d)$ are identified as clusters. The process terminates with the elimination of all links. This algorithm helps the conceptualization of the cluster hierarchy formation and is easily applied to small problems, with about 20 to 30 nodes per graph. A special type of tree structure, the *dendrogram*, is used to visualize hierarchical clustering. It consists of layers of nodes representing clusters which are nested into one another as the threshold (d) for the proximity index is varied. Hence, any horizontal cut of a dendrogram creates a clustering.

3.2. Cluster validity in type III groups

A clustering structure is valid if it is "unusual" in some sense. In this subsection, unusualness is expressed in a statistical framework appropriate to the problem.

In case of random type III exciter injections, from an accelerator with Poisson statistics, the interval ($\delta\tau$) between successive component bursts will be exponentially distributed:

$$P(\delta\tau < \tau) = 1 - \exp(-\frac{\tau}{\delta\tau_{av}}) \tag{4}$$

where $\delta\tau_{av}$ is the average interval for the whole group. If we set τ equal to the threshold (d) then the probability (q) that an interval exceeds the threshold is obtained, while p ($= 1 - q$) will be the probability that the interval is below the threshold.

The probability ($R(k; n; p)$) that a cluster of size at least k (i.e. $k+1$ successive injections with interval less than the threshold d) does not appear, can be calculated recursively (Derman et al 1982, Shantikumar 1982):

$$R(k; n; p) = \sum_{i=n-k}^{n-1} pq^{n-i-1} R(k; i; p) \tag{5}$$

where $k+1$ is the size of the cluster, $n+1$ the size of the group and p, q are calculated from Eq. (4) as functions of the group average interval ($\delta\tau_{av}$) and the threshold (d). Eq. (5) was first derived for the computation of the reliability of a k-consecutive-n:F system which is a system of n units that fails if k (or more) consecutive units fail (Bollinger, 1982, Chiang & Niu 1981).

4. Observations and data reduction

The observations were made with the Multichannel Radiospectrograph of the Space Research Laboratory of the Observatory
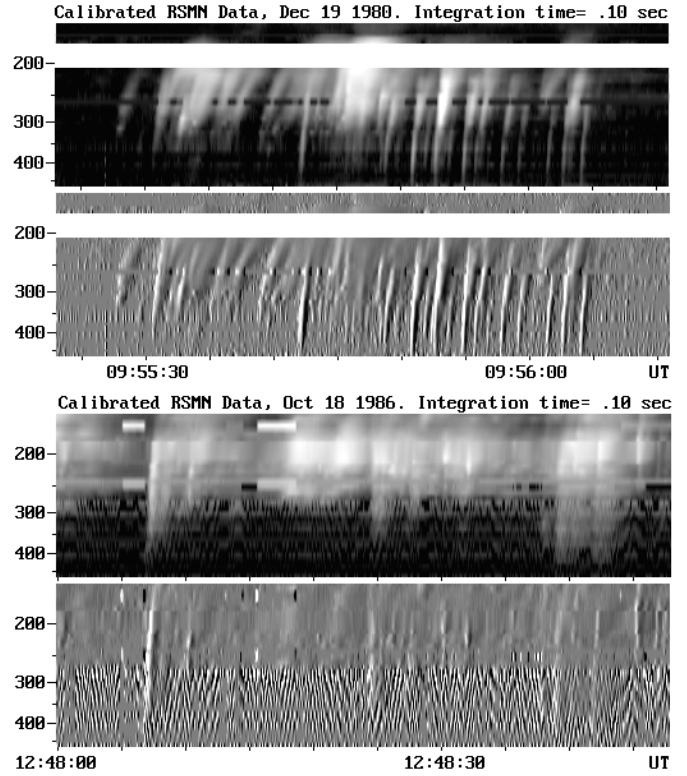
Fig. 1. Dynamic spectra of type III group December 19, 1980 (9:56 UT), and October 18 1986 (12:48 UT) observed with the Multichannel Radiospectrograph of the Space Research Laboratory of the Observatory of Paris. The *top panel* of each spectrum shows the flux and the *bottom* its time derivative.

of Paris in the 450-150 MHz range (Dumas et al, 1982). The output of 120 independent frequency channels was recorded on photographic film; this output is proportional to the logarithm of the antenna temperature, thus increasing the dynamic range of the instrument. Thirty two channels were digitized at a rate of 10 samples/sec and recorded on magnetic tape. Each channel had a 3db bandwidth of 1MHz and their frequencies were logarithmically spaced to compensate for the exponential (hydrostatic) coronal density (and local plasma frequency) variation with height. The data were calibrated in the standard manner (Hillaris et al., 1990).

From the available digital data four type III groups with 10 or more component bursts each were selected for analysis: on December 19, 1980, at 9:56 UT, and on October 18, 1986, at 12:44 UT, 12:48 UT and 13:43 UT. These groups were selected because, on their dynamic spectra, the activity looked steady and stationary. Dynamic spectra, intensity and differential plots of the groups of December 19, 1980 (9:56 UT) and October 18 1986 (12:48 UT) are shown in Fig. 1.

5. Analysis of time profiles

The major problem with the type III groups is that, at least part of the profile of each component is indistinguishable from the overlapping profiles of the others of the same group. In our analysis, the separation of individual bursts was done by fitting the
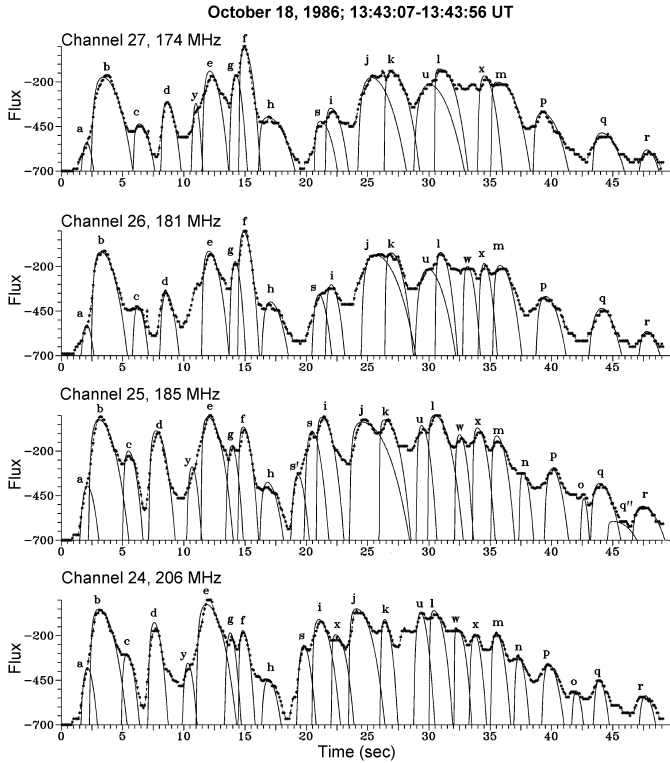
Fig. 2. Profiles of flux vs time for four channels in the 174-206 MHz range for the event of October 18, 1986 13:43 UT. The flux scale is in units of 1/50 db. The thin lines show the fit with Eq. (3) for some individual bursts, identified by letters; we do not show all fitted components in order to avoid confusion.

undisturbed part of each component with the analytical profile of Eq. (3). Only frequency channels with adequate data points were used. This was more difficult in the lower frequencies where the individual burst profiles appeared more diffuse and merged into each other. An example for the event of October 18, 1986 13:43 UT, is shown in Fig. 2.

For each individual burst we estimated the injection time of the corresponding electron beam. Although this parameter enters explicitly in Eq. (3), the scatter of the fitted values over the frequency range is considerable. However, since the duration of type III's increases with time as a result of beam spreading (Hillaris et al 1988, 1990), a more reliable method is to extrapolate the time profile backwards and to determine the time at which its width becomes minimum.

For this purpose we measured the duration of each burst, D, at a number of discrete levels below the local maximum. In Fig. 3 we show examples of plots of the duration of the flux profile, D, as a function of the time of maximum T_m for levels of 1, 1.5, 2, and 3 db's below the peak. For each particular level the points were fitted with a straight line.

If the pulse were instantaneous, the straight lines would all intersect at $D = 0$. However, due to the finite duration of the pulse as well as the observational uncertainties, this is not the case. We therefore used the centroid of the intersections of each two lines as an estimate of the injection time, provided that the

intersections were for $D > 0$. We estimate that the error in this measurement is 0.1 to 0.2 seconds, i.e. comparable to the temporal resolution of the instrument.

The time difference (interval) between the component injection time was used as a proximity index for the detection of clusters within the groups. The cluster formation within the groups, as a function of the proximity index threshold, can be visualized in a dendrogram plot such as the one presented in Fig. 4. For each detected cluster, we computed the average and standard deviation of the inter-arrival time, $\delta\tau$.

6. Results

6.1. Group of December 19, 1980

This group consists of 26 component bursts. The higher frequency range was mostly used in the analysis, since further decomposition of the group profile into component bursts in lower frequencies was not possible because the bursts merged strongly and was not possible to define with confidence unperturbed parts for the fit. The injection times were determined from plots of burst duration vs time (as in Fig. 2) and the interval ($\delta\tau$) between successive injections was computed for each pair. This interval was used as a proximity criterion in the cluster detection process. The hierarchy of subgroups that forms as the threshold decreases is visualized as a dendrogram in Fig. 4. In this graph events with successive inter arrival times ($\delta\tau$) less than a specified value (the threshold, d) are linked together and belong to the same cluster. For a large enough threshold, all events form a single cluster; as the threshold decreases (from right to left in Fig. 4) this single cluster is partitioned, forming a hierarchy of sub-clusters, while the graph assumes a tree like form, hence the name dendrogram.

The analysis of the group and the subgroup parameters is summarized in Table 1, which contains all the information required for the design of the dendrogram. In addition the average and standard deviation of inter-arrival times are given for each cluster with more than four components.

The group forms a single cluster for values of the dissimilarity index (inter arrival time) greater than 3.2 seconds. The average interval between injections is $<\delta\tau> = 1.1 \pm 0.75$ sec. As the threshold decreases to 2.2, two subgroups form: one includes the events {a, e, b, c, y, d, f, g, k, h} with $<\delta\tau> = 0.82 \pm 0.65$ sec and the other contains {i, j, l, m, n, o, p, q, v, r, s, t, w, u, z, x} with $<\delta\tau> = 1.12 \pm 0.59$ sec. For even smaller thresholds three distinct subgroups appear, which retain their identity until the threshold drops to about 1 sec. The first is {a, e, b, c, y, d}, with $<\delta\tau> = 0.46 \pm 0.38$ sec. The second is {l, m, n, o, p} with $<\delta\tau> = 1.05 \pm 0.19$ sec and the third is {s, t, w, u} with $<\delta\tau> = 1 \pm 1$ sec.

We note that the confidence of the three distinct small clusters which retain their identity as the threshold decreases is quite high. From Eq. 5 we computed the probability for a cluster {a, e, b, c, y, d} to appear by chance, which is equal to 30%. Since this result refers to a single clusters, it is only an upper limit of the probability that clusters appear by chance, therefore the confidence of cluster detection is more that 70%.
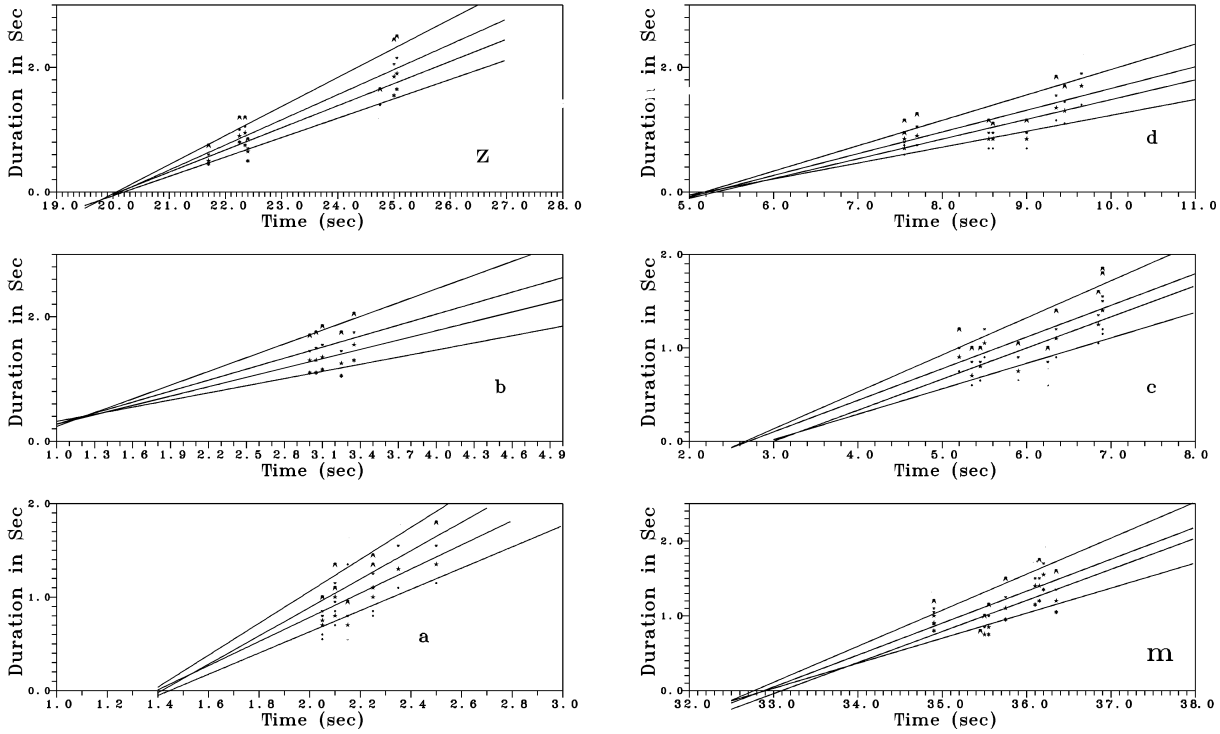
Fig. 3. Plots of the duration of type III burst components (identified by the same letters as in Fig. 2 as a function of time, at four intensity levels below the peak. The intersection of the four straight lines provides an estimate of the injection time. The plots are from the group of October 18, 1986 at 13:43 UT.

Table 1. Cluster analysis of the December 19, 1980 group

Event	Injection time (sec)	$d\tau$ (sec)	Threshold (sec)								
			1.0	1.1	1.3	1.4	1.5	1.8	2.1	2.2	3.2
a	0.9	0.7									
e	1.6	0.1									
b	1.7	0.3	0.46								
c	2.0	0.2	±0.38	0.57	0.57						
y	2.2	1.0		±0.43	±0.43	0.69	0.69	0.69			
d	3.2	1.1				±0.50	±0.50	±0.50	0.82	0.82	
f	5.3	1.4							±0.65	±0.65	
g	6.7	2.1									
k	8.8	0.5									
h	9.3	3.2									
i	12.5	0.5									
j	13.0	1.8									1.1
l	14.8	0.9							1.08	1.16	±0.75
m	15.7	0.9			1.05	1.05	1.05	±0.44	±0.55		
n	16.6	1.3			±0.19	±0.19	±0.19				
o	17.9	1.1								1.12	
p	19.0	2.1								±0.59	
q	21.1	0.5									
v	21.6	1.4									
r	23.0	2.2									
s	25.2	0.8		1.0	1.0	1.0					
t	26.4	0.2		±1.0	±1.0	±1.0	0.84	0.84	0.84		
w	26.6	1.1					±0.49	±0.49	±0.49		
u	27.7	1.5									
z	29.2	0.6									
x	29.8										

Fig. 4. Dendrogram for the event of December 19, 1980, demonstrating the hierarchy of cluster formation for various thresholds. (Thresholds (d) decrease from right to left; as they decrease, clusters are partitioned into sub clusters) Note that the vertical axis of the plot is not to scale, hence the distance between the horizontal lines is not proportional to the interval between successive events

6.2. Group of October 18, 1986, 12:44:36-12:45:46 UT

Three groups recorded by the RSMN on October 18, 1986 were analyzed in the range 226-152 MHz. The first group consists of 45 components; it forms a single cluster for thresholds greater than 3.7 sec with average inter-arrival time of 1.41 ± 0.90 sec.

As the threshold becomes smaller than 3.7 sec two clusters form: one with the first 32 components, $< \delta\tau > = 1.28 \pm 0.77$ sec, and one with the remaining 13, $< \delta\tau > = 1.57 \pm 1.02$ sec. For a threshold equal to 2.80 three clusters, apart from triplets and pairs, form: one with 7 components, $< \delta\tau > = 1.18 \pm 0.77$ sec which retains its identity down to 2.2 sec loosing one component only, one with 25 components $< \delta\tau > = 1.23 \pm 0.70$ sec, which is divided into two smaller clusters (10 and 9 components each, see below) as the threshold decreases, and one with eight components $< \delta\tau > = 1.70 \pm 0.74$ sec which does not retain its identity for lower thresholds. As the threshold decreases further triplets and pairs of bursts start to form. However for threshold down to 2.2 sec three clusters still retain their identity. The first has 6 components, with $< \delta\tau > = 1.00 \pm 0.72$ sec, the second has 10 components with $< \delta\tau > = 1.11 \pm 0.49$ sec and the third has 9 components with $< \delta\tau > = 1.06 \pm 0.58$ sec. The confidence of the large cluster of 22 components is 90%, as computed from Eq. (5).

6.3. Group of October 18, 1986, 12:48:15-12:48:35 UT

This Group consists of 38 component bursts. For values of the inter arrival time than 3.05 sec seconds, the group forms a u

unique cluster with $< \delta\tau > = 0.98 \pm 0.65$ sec. As the interval threshold decreases, two clusters form: one with 28 components, confidence level 72%, $< \delta\tau > = 0.97 \pm 0.58$ sec and another with 9 components, $< \delta\tau > = 0.87 \pm 0.67$ sec. For even smaller threshold of about 1.7 sec, five subgroups (clusters) appear. They consist of 7 bursts, with $< \delta\tau > = 0.85 \pm 0.34$ sec, 8 bursts with $< \delta\tau > = 0.94 \pm 0.41$ sec, 6 bursts with $< \delta\tau > = 0.66 \pm 0.29$ sec, 6 bursts with $< \delta\tau > = 0.62 \pm 0.48$ sec and 7 bursts with $< \delta\tau > = 0.70 \pm 0.32$ sec.

6.4. Group of October 18, 1986, 13:43:08-13:43:57 UT

There were 29 component bursts identified in this group. They form a single cluster for values of the dissimilarity index greater than 4.2 seconds; the average interval between injections is 1.60 ± 1.19 sec. As the threshold decreases to 3.95 sec, subgroups with 12 components, which retains its identity to $d = 2.4$ with a confidence level equal to 77%, with $< \delta\tau > = 1.30 \pm 0.79$ sec and 17 components with $< \delta\tau > = 1.47 \pm 1.10$ sec form. When the threshold drops to 2.9 sec the second subgroup is further divided in two clusters of 8 bursts each and with average interval 1.26 ± 0.83 and 1.18 ± 0.82 sec. Down to a threshold of 2 sec there are still three clusters of 8, 5 and 5 bursts, with average inter arrival times of 1.11 ± 0.58, 1.49 ± 0.40 and 0.83 ± 0.23 sec respectively.

7. Summary and conclusions

Using a simple, free streaming model for the propagation of energetic electrons in open or closed magnetic field configurations and the assumption of a power law dependence of the electromagnetic emission on the electron density of the beam, we extrapolated component bursts of type III groups in order to estimate their injection time. This method of extrapolation *backward in time*, presented here for the first time, can reduce an observed type III (or even N, J, U) group into a single time series of *pulses* tracing thus the temporal variations of the *source* of the group.

Clustering algorithms were used for the analysis of the sequence of consecutive injections; we show that there is a tendency of hierarchical subgroup formation within the type III groups. This clustering tendency was observed in the time scales of 4.2 seconds to 1 second. In the case of pulsed mode burst organization, one would expect a single cluster for thresholds above $< \delta\tau > + \sigma(\delta\tau)$ (where $\sigma(\delta\tau)$ stands for standard deviation of $\delta\tau$) and mostly isolated bursts below $< \delta\tau > - \sigma(\delta\tau)$, with a rather abrupt transition since, in a periodic process we expect the standard deviation of the inter arrival time to be very small. ($\sigma(\delta\tau) \ll < \delta\tau >$). If the injections were random, on the other hand, then clusters could occasionally form but not to the extend presented here as analysed in the previous section.

The clustering tendency thus observed and quantified seems to be consistent with similar tendencies observed in simulations of "*flaring sites*" by Vlahos, et al (1995), Lu and Hamilton 1991, Lu at al 1993, Georgoulis and Vlahos, 1996. We note that in all previously mentioned variants of the self organized critical

model, for the statistical flare, the emphasis of the analysis is on the magnitude of the energy release, hence the observed clusters are spatial. However the energy release takes place within a number of simulation time steps where a flaring element *loads* each adjacent element with surplus magnetic flux some of which are bound to flare at the next time step until the system relaxes. Hence the energy release is associated with a temporal cluster of elementary energy releases. These elementary releases are expected to energise the *elementary injections* contributing to both type III groups and isolated bursts (Vlahos 1994, Vlahos & Raoult 1995). It should be noted though that, each pulse obtained in our backward extrapolation might correspond to a number of elementary injections in rapid succession. This is a consequence of the temporal resolution of the instrument (1/10 sec), which makes the discrimination of elementary injections of shorter time separation impossible. Due to the intrinsic complexity of the acceleration site there is always a possibility that two or more disjoint clusters of elementary injections might appear as a single cluster of pulses. However, assuming that for each "*quiescent element*" the time to "*flaring*" is long enough so that disjoint regions never flare simultaneously, which may well be the case in the weakest flaring sites, our approach provides a reasonable approximation.

Based on the above, some variant of the statistical flare model seems to be the most appropriate way to interpret of the present results. This implies a process of proximity self organization in the source of the groups which is consistent with the idea of triggering and energization of neighboring flare elements or elementary flares.

References

Aschwanden M., 1991, In: Schmieder, Priest (eds.) Flares 22 Workshop. Dynamics of Solar Flares. 55
Aschwanden M., Benz A.O., Montello M.L., 1994, ApJ 431, 432
Aschwanden M., Benz A.O., Schwartz R., Stehling W., 1990, Solar Phys. 130, 39
Aschwanden M., Benz A.O., Dennis B.R., Gaizauskas V., 1993, ApJ 416, 857
Aschwanden M., Benz A.O., Dennis B.R., Kundu M., 1994, ApJS 90, 631
Aschwanden M., Montello M.L., Dennis B.R., Benz A.O., 1995, ApJ 440, 394

Bastian T.S., Vlahos L., 1996, In: Trottet G. (ed.) Coronal Physics from Radio and Space Observations. Lecture Notes in Physics 483, 68
Benz A.O., Treumann R., Vilmer N., et al., 1982, A&A 108, 161
Bhatnagar P.L., Gross E.P., Krook M., 1954, Phys Rev. 94, 511
Bollinger R.C., 1982, IEEE Trans. Rel., R31, 444
Chiang D. I., Niu S.C., 1981, IEEE Trans. Rel., R30, 87
Dawson J.M., Oberman C., 1962, Phys. Fluids 5, 517
Derman C., Lieberman G.J., Ross S. M., 1982, IEEE Trans. Rel., R31, 57
Dumas G., Caroubalos C., Bougeret J-L., 1982, Solar Phys. 81, 383
Fitzenreiter R., Evans L., Lin R., 1976, Solar Phys. 46, 437
Georgoulis M., Vlahos L., 1996, ApJ 469, L135
Goldstein M., Smith R., Papadopoulos K., 1979, ApJ. 234, 683
Hillaris A., Alissandrakis C., Vlahos L., 1988, A&A 195, 301
Hillaris A., Alissandrakis C., Caroubalos C., Bougeret J-L., 1990, A&A 229, 216
Isliker H., 1996, A&A 310, 672
Jain K.A., Dubes R.C., 1988, Algorithms for Clustering Data. Prentice Hall
Lu E., Hamilton R.J., 1991, ApJ 380, L89
Lu E., Hamilton R.J., McTiernan J.M., Bromund K., 1993, ApJ 412, 841
MacKinnon A.L., MacPherson K.P., Vlahos L., 1996, ApJ 310, L9
Mangeney A., Pick M., 1989, A&A 224, 242
Muschieti L., Goldman M.V., Newman D.L., 1985, Solar Phys. 96, 181
Papadopoulos K., 1975, Phys. Fluids 18, 1759
Papadopoulos K., 1977, Rev. Geophys. Space Phys. 15, 173
Papadopoulos K., Freud H.P., 1979, NRL Memo Rept. 3992
Papadopoulos K., Goldstein M., Smith R., 1974, ApJ 190, 175
Pick M., van den Oord G. & H., 1990, Solar Phys. 130, 83
Poquerusse M., 1977, A&A 56, 251
Poquerusse M., Bougeret J-L., Caroubalos C., 1984, A&A 136, 10
Roelof E.G., Pick M., 1989, A&A 210, 417
Shantikumar J.G., 1982, IEEE Trans. Rel., R31, 442
Smith R., Goldstein M., Papadopoulos K., 1979, ApJ 234, 348
Stepanova N.A., Bazelyan L.L., Abranin E.P., et al., 1995, Solar Phys. 156, 131
Vlahos L., 1991, In: Schmieder, Priest (eds.) Flares 22 Workshop. Dynamics of Solar Flares. 91
Vlahos L., 1993, Adv. Space Res. 13, 161
Vlahos L., Rowland H., 1984, A&A 139, 263
Vlahos L., Raoult A., 1995, A&A 296, 844
Vlahos L., Georgoulis M., Kluiving R., Paschos P., 1995, A&A 299, 897
Vilmer N., Trotter G., 1996, In: Trottet G. (ed.) Coronal Physics from Radio and Space Observations. Lecture Notes in Physics 483, 28
Wild J.P., 1950, Australian J. Sci.Res. A3, 339
Wild J.P., 1963, In: Evans J.W. (ed.) The Solar Corona. Academic Press, New York, p. 115
Yurovsky Yu., Magun A., 1996, Solar Phys. 166, 433
Zacharov V.E., 1972, Soviet Phys. JETP 35, 908
Zhao R-Y., Mangeney A., Pick M., 1991, A&A 241, 183
Zheleznyakov V.V., Zaitsev V.V., 1970, Soviet Astron. 14, 250